2010

Computational Structural Modelling of Coronary Stent Deployment: A Review

David Martin
Technological University Dublin, david.martin@tudublin.ie

Fergal Boyle
Technological University Dublin, fergal.boyle@tudublin.ie

Recommended Citation

Martin, D., Boyle, F.: 'Computational structural modelling of coronary stent deployment: a review', Computer Methods in Biomechanics and Biomedical Engineering (2011) Volume: 14, Issue: 4, Pages: 331-348. PubMed: 20589544 doi:10.1080/10255841003766845

Computer Methods in Biomechanics and Biomedical Engineering
Vol. 00, No. 0, 2010, 1–18

Taylor & Francis
Taylor & Francis Group

Computational structural modelling of coronary stent deployment: a review

David Martin* and Fergal J. Boyle

Department of Mechanical Engineering, Dublin Institute of Technology, Dublin 1, Ireland

(*Received 4 November 2009; final version received 10 March 2010*)

The finite element (FE) method is a powerful investigative tool in the field of biomedical engineering, particularly in the analysis of medical devices such as coronary stents whose performance is extremely difficult to evaluate *in vivo*. In recent years, a number of FE studies have been carried out to simulate the deployment of coronary stents, and the results of these studies have been utilised to assess and optimise the performance of these devices. The aim of this paper is to provide a thorough review of the state-of-the-art research in this area, discussing the aims, methods and conclusions drawn from a number of significant studies. It is intended that this paper will provide a valuable reference for future research in this area.

Keywords: cardiovascular disease; stent; restenosis; finite element analysis; review

1. Introduction

At present, coronary artery disease (CAD) is one of the leading causes of death and disability in the developed world. According to the American Heart Association, in 2005 alone, approximately 445,687 deaths in the USA were attributable to CAD, representing 20% of all deaths in the USA that year. CAD occurs due to the development of atherosclerotic plaques within the coronary arteries that supply oxygen and vital nutrients to the heart muscle. Several risk factors have been identified which contribute to the progression of this disease including smoking, hypertension, diabetes mellitus and high cholesterol (Lloyd-Jones et al. 2009). As an atherosclerotic plaque increases in size it can significantly restrict the flow of blood through a coronary artery, often resulting in myocardial infarction.

In the 1970s, percutaneous transluminal coronary angioplasty (PTCA) was introduced as a minimally invasive treatment for CAD. A typical PTCA procedure involves the use of X-ray guidance to deliver a balloon-tipped catheter to the diseased section of an artery. Once in place, the catheter balloon is inflated to a nominal pressure and compresses the atherosclerotic plaque against the arterial wall, improving the flow of blood to the heart. Although treatment with PTCA generally results in high clinical success rates, many patients redevelop the initial symptoms over 6–12 months. This re-narrowing of the treated artery is caused by restenosis, the principal limitation of this procedure. Restenosis following PTCA is primarily attributed to the elastic recoil of the vessel wall and is observed in 30–40% of treated patients (Fischman et al. 1994).

In the 1980s, bare-metal stents (BMSs) were introduced to reduce rates of restenosis associated with PTCA. A BMS is a small, cylindrical, wire mesh device that is crimped and loaded upon a balloon-tipped catheter and delivered to the diseased section of the artery. When the catheter balloon is inflated, the atherosclerotic plaque is compressed against the arterial wall as with PTCA and the metallic stent is expanded to a nominal diameter through plastic deformation. Following deployment, the stent remains within the artery minimising elastic recoil and maintaining vessel patency post treatment. Again, though treatment with a BMS will generally result in extremely favourable initial clinical results, re-narrowing of the treated artery is typically observed in 20–30% of patients over 6–12 months (Fischman et al. 1994; Vivek and Stanley 2003). This re-narrowing of the treated artery is due to in-stent restenosis (ISR). ISR is caused by neointimal hyperplasia within the vessel and is defined as a loss of $\geq 50\%$ of the initial gain in lumen diameter achieved through stent placement.

In recent years, a number of drug-eluting stents (DESs) have been introduced in an attempt to address the problem of ISR. A DES typically consists of a BMS which has been coated in a formulation of anti-restenotic agents and suitable carrier materials. The drugs commonly employed are known to interrupt the key cellular and molecular processes associated with neointimal hyperplasia. To date, clinical evaluation has overwhelmingly proven the superiority of DESs over BMSs with reported reductions in ISR rates of between 60 and 80% (Morice et al. 2002; Moses et al. 2003; Stone et al. 2004; Ong et al. 2006). Despite the success of DESs in the reduction of rates of ISR, concerns have arisen over the long-term biocompatibility of these

*Corresponding author. Email: david.martin@dit.ie

ISSN 1025-5842 print/ISSN 1476-8259 online

DOI: 10.1080/10255841003766845
http://www.informaworld.com

devices due to cases of late adverse clinical events such as stent thrombosis (Daemen et al. 2007; Finn et al. 2007). As such, research in this area is currently centred on the identification and evaluation of improved stent designs and, the development of biocompatible and bioabsorbable stent materials.

As the performance of a stent deployed within a coronary artery can be difficult and expensive to evaluate experimentally, computational numerical methods have emerged as powerful tools in the assessment of stent design and performance. In recent years, numerical models utilising computational fluid dynamics and mass transport theory have been developed to investigate both blood flow within stented arteries and drug-transfer from a DES (LaDisa et al. 2002, 2004, 2005; Pontrelli and de Monte 2007; Balossino et al. 2008; Zunino et al. 2009). Furthermore, due to strong links between levels of vascular injury induced during stent deployment and the degree of ISR observed at follow-up, a number of studies have utilised the finite element (FE) method to investigate the structural properties of stents and their biomechanical impact on the coronary artery during deployment. As a result of rapidly increasing levels of computational power and the development of robust FE applications in recent years, the level of complexity and sophistication involved in these studies has risen considerably. The aim of this paper is to present a thorough review of the FE analysis of coronary stent deployment, highlighting the contribution of a number of key studies over the last decade.

In Section 1 of this paper, the major steps involved in an FE analysis of stent deployment are introduced and discussed. In the following two sections, several key studies involving the FE analysis of both stent-free expansion (Section 2) and stent deployment within a vessel (Section 3) are presented and in Section 4 conclusions are drawn and future prospects in the numerical analysis of coronary stents are briefly discussed. Over 50 studies representing the most widely cited works in this field were evaluated during the preparation of this review and it is intended that this paper will prove a valuable reference tool for future research in this area.

2. FE method for the analysis of stent deployment

2.1 Introduction

The FE method is a numerical technique used to obtain approximate solutions for systems of differential or integral equations applied over domains of complex shape. This process involves the discretisation of the domain of interest into a number of smaller sub-domains of simple shape known as FEs. Each of these elements consists of a series of control points, known as nodes, and the entire discretised domain is referred to as an FE mesh. In a typical structural analysis, the individual elements can be analysed using simple stress–strain relations and, through the consideration of equilibrium at each element interface and known boundary and loading conditions, a set of algebraic equations can be derived. The solution of these equations yields generalised nodal displacements which can be used to determine nodal values of both stress and strain. Assuming that certain numerical requirements have been satisfied, the solution obtained should approximate the exact physical solution.

A typical FE analysis of stent deployment involves a number of important pre-processing stages. The first of these stages involves the generation of FE meshes for each component in the analysis. These FE meshes are typically obtained directly from computer-generated solid models using mesh generation or discretisation algorithms. Material properties for each individual component must then be defined and appropriate boundary and loading conditions must be applied. Finally, a suitable solution methodology must be chosen. These steps are discussed in further detail in the following sections.

2.2 Solid model and FE mesh generation

The first stage in any FE analysis involves the generation of suitable solid models for each of the individual components being investigated. In an FE analysis of stent deployment, solid models of a stent, a catheter balloon and a stenotic artery may be required. Today, most commercially available FE packages facilitate solid model generation and also support models generated and imported from a number of stand-alone computer-aided design packages. Once generated, these solid models must be discretised into satisfactory FE meshes.

Due to the complicated geometrical design of most stents and because the majority of commercially available stents are subject to strict patent claims restricting the distribution of information regarding their geometrical features, the generation of a solid model of a stent is not a straightforward task. One strategy that has been utilised to develop FE meshes of a number of stent designs involves cutting an actual stent along its longitudinal axis and measuring important geometrical properties such as strut width, thickness and length using a microscope. Using these measurements, a model of the planar stent geometry can be accurately defined within an FE package. This model can then be discretised into a suitable mesh and rotated into its cylindrical configuration by coordinate transformation (Figure 1). A second strategy that has been adopted in recent years involves the use of X-ray tomography to generate a detailed 3D model of the stent. Using this methodology, highly accurate FE meshes of complex stent designs can be generated. Stent solid models are generally discretised using solid elements.

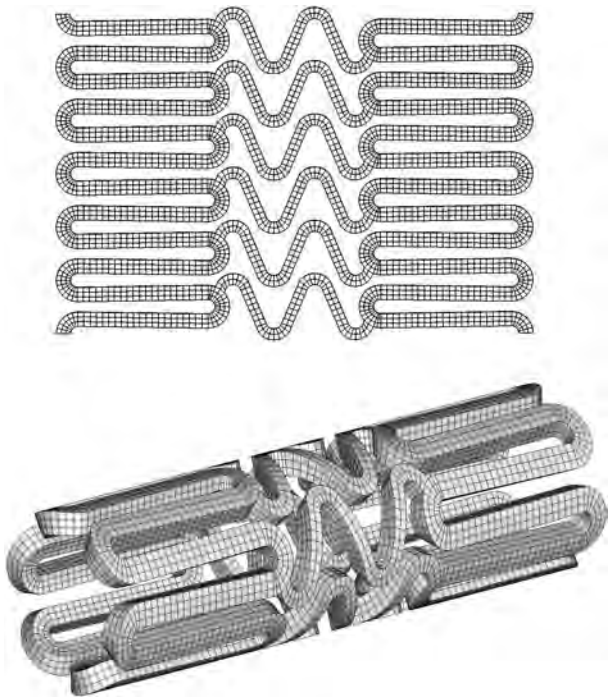

Figure 1. 'Wrapping' of planar stent geometry (top) into its cylindrical configuration (bottom).

In practice, a stent is crimped and loaded upon a balloon that is both tapered and folded onto a catheter. In studies in which the expansion of the stent has been simulated through balloon dilation, the catheter balloon is generally modelled as an idealised cylindrical surface and discretised using shell elements. In studies that have evaluated the expansion of a stent within normal and stenotic arteries, the artery is generally modelled as an idealised cylinder and discretised using solid elements while the stenosis is generally modelled as an idealised, parabola-shaped plaque and also discretised using solid elements.

2.3 Material properties

Before any FE analysis can be performed, the material behaviour of each component in the analysis must be defined using appropriate mathematical material models. Coronary stents are generally manufactured from biologically inert metallic materials such as medical grade 316L stainless steel. The behaviour of these materials is elastic–plastic in nature and their response to uniaxial loading is highly non-linear. In the majority of studies to date, the stent material is simplified as a homogeneous, isotropic material and its behaviour is typically defined using bilinear and multi-linear plasticity models with isotropic hardening. These plasticity models are incorporated in most commercially available FE packages and are generally defined using data obtained from experimental tests. In order to simulate the expansion of the stent by balloon dilation, the material behaviour of the balloon must also be defined. Angioplasty balloons are usually manufactured from materials such as polyethylene terephthalate and polyamide, and their behaviour is typically modelled using linear elastic material models based on data provided by the manufacturer.

Predicting the material behaviour of arterial tissue has proven a difficult task due to the non-linear, anisotropic, stress-stiffening nature of the material. In the majority of studies, the arterial tissue is simplified as a homogeneous, isotropic and incompressible material and its behaviour is defined using a hyperelastic constitutive model. A hyperelastic material is an ideally elastic material for which the stress–strain relationship is derived from a strain-energy function. A strain-energy function is defined as a measure of the energy stored in a material as a result of its deformation and is generally fit to data obtained from experimental testing of arterial tissue. Most commercially available FE packages include a number of hyperelastic constitutive material models and suitable curve-fitting applications capable of capturing the behaviour of biological materials.

2.4 Boundary and loading conditions

For valid results, an FE mesh should only be subjected to realistic boundary and loading conditions that are representative of the actual conditions in question. For the analysis of stent deployment, the stent must be free to expand and contract in the radial and longitudinal directions yet fixed such that rigid-body motions are prevented. Generally, a small number of nodes in each of the discretised components in the analysis are constrained from movement in a very specific number of directions to avoid any rotational or translational movement.

In terms of loading conditions, stent expansion is typically achieved through displacement control, pressure control or through explicit modelling of a balloon. To date, studies in which stent expansion has been achieved through displacement control have involved the expansion of an analytical surface within the stent, while studies in which stent expansion has been achieved through pressure control have involved the application of a pressure load on the inner surface of the stent. When the presence of a catheter balloon is included in the analysis, the expansion of the stent is generally achieved through the application of a pressure load on its inner surface. As the balloon expands, contact conditions between it and the stent force the expansion of the stent.

2.5 Solution

The final step in the pre-processing stage of a structural FE analysis is the selection of a solution methodology capable of calculating the nodal displacements, stresses and strains. To date, studies on stent deployment have used

either static or explicit analysis. A non-linear static structural analysis does not consider dynamic effects; however, due to the presence of large deformations in the analysis, a solution is generally obtained over a series of sub-steps to ensure numerical stability. During each sub-step, a fraction of the loading conditions is applied and the final solution is obtained in a piecewise fashion. Most commercially available FE packages incorporate a Newton–Raphson iterative solver for solving non-linear static structural problems (Mac Donald 2007). The general equation solved in a non-linear static analysis is

$$[K]\{\mathbf{U}\} = \{\mathbf{F}\}, \tag{1}$$

where $[K]$ is the global stiffness matrix; $\{\mathbf{U}\}$ is the nodal displacement vector and $\{\mathbf{F}\}$ is the load vector.

A non-linear explicit analysis is another approach often used in FE modelling of stent deployment. The general equation solved in a non-linear explicit analysis is

$$[M]\{\ddot{\mathbf{U}}\} + [C]\{\dot{\mathbf{U}}\} + [K]\{\mathbf{U}\} = \{\mathbf{F}(t)\}, \tag{2}$$

where $[M]$ is the global mass matrix; $\{\mathbf{F}(t)\}$ is the time-dependant load vector;, $[C]$ is the global damping matrix; $[K]$ is the global stiffness matrix and $\{\mathbf{U}\}, \{\dot{\mathbf{U}}\}$ and $\{\ddot{\mathbf{U}}\}$ are the nodal displacement, velocity and acceleration vectors, respectively.

In an explicit analysis, the loading conditions are applied over a number of time steps and a solution is obtained through a time-integration procedure. During explicit time integration, the solver will increment a time step and determine if the loads applied to the structure are in equilibrium with the internal forces. Nodal accelerations are calculated directly from Newton's second law and a solution is obtained on an element-by-element basis (Mac Donald 2007).

3. Review of FE analysis of stent deployment

Due to strong links between levels of vascular injury induced during stent deployment and ISR rates and in order to investigate the mechanical behaviour of coronary stents, the FE method has been utilised in a large number of studies to evaluate stent deployment. In the following sections, a number of key studies in this area have been categorised as either analyses of the deployment characteristics of stents during free expansion or analyses of the biomechanical impact of stents when deployed within a vessel, and are presented and discussed in Section 3.1 and 3.2, respectively.

3.1 FE analysis of the free expansion of coronary stents

In the context of stent analysis, the term free expansion is used to refer to the expansion of a stent without any outside impedance. To date, several studies have been carried out to investigate how geometrical properties, material properties and deployment methods affect the expansion characteristics of various stent designs (Whitcher 1997; Brauer et al. 1999; Dumoulin and Cochelin 2000; Etave et al. 2001; Tan et al. 2001; Chua et al. 2002, 2003, 2004a; Migliavacca et al. 2002, 2005; Stolpmann et al. 2003; McGarry et al. 2004; Petrini et al. 2004; Savage et al. 2004; Gu et al. 2005; Hall and Kasper 2006; Wang et al. 2006; De Beule, Mortier, Belis et al. 2007; De Beule, Mortier, Van Impe et al. 2007; De Beule et al. 2008; Donnelly et al. 2007; Wu et al. 2007a; Xia et al. 2007; Ju et al. 2008; Lim et al. 2008; Mortier et al. 2008; Li et al. 2009). A number of these studies which represent significant contributions to research in this field are discussed and summarised in this section (Table 1).

Dumoulin and Cochelin (2000) presented results from one of the first studies of stent deployment to utilise the FE method. The aim of this study was to evaluate the deployment characteristics and long-term performance of a Palmaz–Schatz stent (Johnson & Johnson, New Brunswick, NJ, USA) following free expansion. The simplest of the numerical models considered in this study was based on the repeating unit cell of the Palmaz–Schatz stent (Figure 2) and its expansion was achieved through the application of a pressure load on its inner surface. The decision to consider only the repeating unit cell of the stent was justified after the investigators examined the *in vitro* expansion of a Palmaz–Schatz stent, concluding that, except at its ends, it was almost uniformly expanded and evenly dilated. Rates of radial and longitudinal recoil were calculated and the results were validated against the manufacturer's data. Further numerical models were then generated to assess the buckling and fatigue life of the Palmaz–Schatz stent. This study represents one of the first attempts to evaluate the deployment characteristics of a coronary stent using the FE method.

One year later, Etave et al. (2001) presented results from a study of the deployment characteristics of both tubular and coil stents following free expansion. The tubular stent was an approximation of the Palmaz–Schatz stent, while the coil stent was an approximation of the Freedom stent (Global Therapeutics Inc., Broomfield, CO, USA). Stent expansion was achieved through the application of a displacement-driven loading condition upon the nodes of the stent and a number of expansion characteristics such as the deployment pressure, elastic recoil, stress–strain distributions and foreshortening for both stents were evaluated. Additional simulations were carried out to evaluate the conformability and the resistance to compression for both stents. This study represents one of the first comparative studies of two different stents carried out using the FE method.

Migliavacca et al. (2002) presented results from a study carried out to investigate the effect of geometrical parameters such as metal-to-artery surface ratio, strut

Table 1. Finite element studies of stent-free expansion.

Years	Authors	Study title	Modelling parameters	Study aims and conclusions
2000	Dumoulin and Cochelin (2000)	Mechanical behaviour modelling of balloon expandable stents	*Stent model*: Palmaz–Schatz stent *Stent material model*: true stress–strain curve based on properties of 316L stainless steel *Solver type*: implicit (ABAQUS©/Standard)	*Aim*: to investigate the deployment characteristics and long-term performance of a Palmaz–Schatz stent following free expansion *Conclusions*: numerical results were validated against experimental data in the literature proving that stent-free expansion may be accurately simulated using the FE method
2001	Etave et al. (2001)	Mechanical properties of coronary stents determined by FE analysis	*Stent model*: Palmaz–Schatz and Freedom stents *Stent material model*: true stress–strain curve based on properties of 316L stainless steel *Solver type*: implicit (ABAQUS©/Standard)	*Aim*: to compare the deployment characteristics of tubular and coil stents following free expansion *Conclusions*: several deployment characteristics of different stent designs may be investigated using the FE method
2002	Migliavacca et al. (2002)	Mechanical behaviour of coronary stents investigated through the FE method	*Stent model*: Palmaz–Schatz, Carbostent and Multi-Link Tetra stents *Stent material model*: elastic–plastic model based on properties of 316L stainless steel *Solver type*: implicit (ABAQUS©/Standard)	*Aim*: to investigate the effect of geometrical parameters on the deployment characteristics of a Palmaz–Schatz stent and to compare this with two next-generation stents *Conclusions*: stent metal-to-artery surface ratio has a significant influence on rates of radial/longitudinal recoil and dog-boning during free expansion
2004	Chua et al. (2004a)	Effects of varying the slotted tube (stent) geometry on its expansion behaviour using FE method	*Stent model*: Palmaz–Schatz stent *Stent material model*: elastic–plastic model based on properties of 304 stainless steel *Balloon model*: ideal cylindrical balloon *Balloon material model*: hyperelastic model based on properties of polyurethane rubber *Solver type*: explicit (ANSYS©/LS-DYNA)	*Aim*: to investigate the effect of geometrical parameters on the expansion characteristics of a Palmaz–Schatz stent following deployment by balloon dilation *Conclusions*: number, width and length of stent cells have a minor effect on the expanded diameter and foreshortening of the device but a significant effect on the rate of elastic recoil
2004	Petrini et al. (2004)	Numerical investigation of the intravascular coronary stent flexibility	*Stent model*: Carbostent and Bx-Velocity stents *Stent material model*: elastic–plastic model based on properties of 316L stainless steel *Solver type*: implicit (ABAQUS©/Standard)	*Aim*: to compare the flexibility of the Carbostent and Bx-Velocity stents in their unexpanded/expanded configurations *Conclusions*: the Bx-Velocity stent exhibits higher flexibility compared to the Carbostent, with both stent models exhibiting lower flexibility in their unexpanded configurations
2004	McGarry et al. (2004)	Analysis of the mechanical performance of a cardiovascular stent design based on micro-mechanical modelling	*Stent model*: repeating unit cell of NIR stent *Stent material model*: macroscopic/microscopic models based on properties of 316L stainless steel *Solver type*: implicit (ABAQUS©/Standard)	*Aim*: to compare and contrast the deployment characteristics of a 2D repeating unit cell of the NIR stent using macroscopic and microscopic material models *Conclusions*: micro-scale material models may be more suitable for defining the material properties of stents
2005	Migliavacca et al. (2005)	A predictive study of the mechanical response behaviour of coronary stents by computer modelling	*Stent model*: Bx-Velocity stent *Stent material model*: elastic–plastic model based on properties of 316L stainless steel *Solver type*: implicit (ABAQUS©/Standard)	*Aim*: to compare the deployment characteristics of both numerically modelled and actual Bx-Velocity stents during free expansion *Conclusions*: modelling of the catheter balloon is required to accurately capture the transient deployment characteristics of a stent during free expansion

Table 1 – *continued*

Years	Authors	Study title	Modelling parameters	Study aims and conclusions
2006	Hall and Kasper (2006)	Comparison of element technologies for modelling stent expansion	*Stent model*: Bx-Velocity stent *Stent material model*: elastic–plastic model based on properties of 316L stainless steel *Solver type*: implicit (ABAQUS©/Standard)	*Aim*: to compare and contrast the performance of several FE types for accurate and efficient numerical analysis of stent-free expansion *Conclusions*: compared to solid and shell elements, beam elements are capable of predicting similar maximum and minimum stresses along a stent at significantly reduced computational costs
2006	Wang et al. (2006)	Analysis of the transient expansion behaviour and design optimisation of coronary stents by FE method	*Stent model*: study-specific stent designs *Stent material model*: elastic–plastic model based on properties of 316L stainless steel *Balloon model*: ideal cylindrical model *Balloon material model*: linear elastic model based on 'virtual' material properties *Solver type*: implicit (ANSYS©)	*Aim*: to investigate the effect of stent and balloon geometrical parameters on the transient behaviour of two study-specific stents during free expansion
2008	De Beule et al. (2008)	Realistic FE-based stent design: the impact of balloon folding	*Stent model*: Bx-Velocity stent *Stent material model*: elastic–plastic model based on properties of 316L stainless steel *Balloon model*: cylindrical and tri-folded balloons *Balloon material model*: linear elastic model based on material properties of duralyn *Solver type*: explicit (ABAQUS©/Explicit)	*Aim*: to compare the transient behaviour of a Bx-Velocity stent during free-expansion simulated by three different loading scenarios *Conclusions*: modelling of the tri-folded nature of catheter balloons is required to accurately capture the transient deployment characteristics of a stent driven by the initial unfolding of the catheter balloon
2008	Lim et al. (2008)	Suggestion of potential stent design parameters to reduce restenosis risk driven by foreshortening or dog-boning due to non-uniform balloon-stent expansion	*Stent model*: Palmaz–Schatz, Texan, MAC Standard, MAC Q23, MAC Plus, Coro flex and RX Ultra Multi-Link stents *Stent material model*: elastic–plastic model based on properties of 316L stainless steel *Balloon model*: tri-folded balloon *Balloon material model*: linear elastic model based on material properties of polypropylene *Solver type*: implicit and explicit (ABAQUS©/Standard and Explicit)	*Aim*: to investigate the deployment characteristics of several stents for the identification of specific design parameters capable of reducing ISR driven by foreshortening and dog-boning *Conclusions*: foreshortening and dog-boning of stents is closely correlated with the configuration of the unit cells, link members, distal geometry and morphology of the stent design

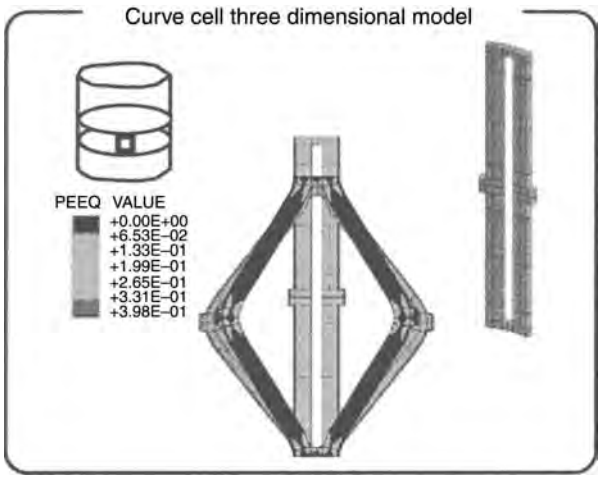

Figure 2. Finite element analysis of the repeating unit cell of a Palmaz–Schatz stent (Johnson & Johnson; Dumoulin and Cochelin 2000).

thickness and cell length on the deployment characteristics of a Palmaz–Schatz stent. The performance of the Palmaz–Schatz stent was then compared to two next-generation stents: the Carbostent (Sorin Biomedica, Saluggia, Italy) and Multi-Link Tetra (Guidant, Indianapolis, IN, USA) stents. The expansion of each stent was achieved through the application of a pressure load on its inner surface and it was observed that geometrical parameters had a significant influence on the deployment characteristics of the Palmaz–Schatz stent following free expansion. In particular, a lower metal-to-artery surface ratio was associated with higher rates of radial and longitudinal recoil and lower rates of dog-boning (stronger radial expansion at the extremities of the stent with respect to the mid-section of the stent). The deployment characteristics of the two next-generation stents following free expansion were also discussed. This study clearly demonstrates the potential of the FE method in the optimisation of stent designs and also represents one of the first attempts to investigate the deployment characteristics of next-generation stents.

Chua et al. (2004a) presented results from a similar study carried out to investigate the effect of geometrical parameters such as the number, width and length of individual stent cells on the deployment characteristics of a Palmaz–Schatz stent following free expansion. In this study, however, the expansion of the stent was achieved through the application of a pressure load on the inner surface of an idealised cylindrical balloon. It was observed that, although varying the number, width and length of the stent cells had only minor effects on the expanded diameter and foreshortening of the stent, it had a major influence on the rate of elastic recoil which decreased as the number of cells and the regularity of their distribution was increased. This study represents one of the first efforts to model the expansion of a stent through balloon dilation and again highlights the potential of the FE method in the optimisation of stent design.

In the same year, Petrini et al. (2004) presented results from a study carried out to compare the flexibility of two next-generation stents in both their unexpanded and expanded configurations. The stents considered were based on a section of the Carbostent and Bx-Velocity (Johnson & Johnson) stents and consisted of two strut segments connected by bridging or link members. This simplification was justified by the investigators through the observation that, in sufficiently curved vessels, the stresses induced on the stent cause it to behave as a series of rigid bodies (the strut segments) connected by individual hinges (the bridging members). To measure the flexibility of the stents in both their unexpanded and expanded configurations, a fixed angular rotation was applied at the extremities of each stent model. Results, expressed in terms of a bending moment-curvature index, demonstrated a different response for the two stents. In particular, the Bx-Velocity stent was associated with a higher degree of flexibility while lower levels of flexibility were observed for both stents in their expanded configurations. According to the authors, the main limitation of this study is the absence of the delivery system in the analysis of the unexpanded stent models. Experimental testing of manufacturer-mounted stents has shown that the presence of a delivery catheter has a significant influence on stent flexibility (Dyet et al. 2000).

AlsoMcGarry et al. (2004) presented results from a study carried out to evaluate the deployment characteristics of a 2D approximation of the repeating unit cell of the NIR stent (Boston Scientific, Natick, MA, USA) during free expansion. The aim of the study was to compare the performance of the unit cell when its material properties were defined using either macroscopic or microscopic mathematical material models. It was argued by the authors that since the typical dimensions of a stent strut are of a similar order of magnitude to the average grain size for stainless steel, a crystal plasticity material model may be more suitable than classic plasticity material models for the numerical analysis of coronary stents. Expansion, recoil and cyclic loading of the unit cell were achieved through the application of displacement and pressure loads at specific nodes within the unit cell. It was observed that the crystal plasticity material model was capable of predicting non-uniform and localised stress–strain fields where the classic plasticity material model could not. The results of this study suggest the possible benefits of using micro-scale material models in the FE analysis of coronary stents though, according to the authors, full 3D modelling should be performed to improve the accuracy of the measured deployment characteristics and also to assess the accuracy of results obtained from the 2D analysis.

Migliavacca et al. (2005) presented results from a study carried out to compare the deployment characteristics of both numerically modelled and real Bx-Velocity stents during free expansion. Using the FE method, the expansion of the modelled stent was achieved through the application of a pressure load on its inner surface, while the expansion of the real stent was achieved through balloon dilation. It was observed that although the modelled stent accurately predicted the initial expansion of the real stent, the behaviour of the modelled stent when subject to higher pressure loads was not descriptive when compared to that of the real stent (Figure 3). It was concluded by the authors that the omission of a balloon in the numerical analysis was the decisive element in interpreting these discrepancies and that its presence should not be neglected in future studies.

Hall and Kasper (2006) presented results from a study carried out to compare the performance of several FE element types for the accurate and efficient numerical analysis of stent deployment. The stent considered was an approximation of the Bx-Velocity stent and in total six different numerical models were generated using variations of 3D solid and 2D shell and beam elements. The expansion of each stent was achieved through the application of a displacement-driven loading condition upon a cylindrical analytical surface. It was observed that each of the element types ensured a similar response despite differences in the dimensionality of the numerical models. It was also noted that, compared to the shell and solid elements, the beam elements were capable of predicting similar maximum and minimum values of stress and strain at identical locations on the stent while significantly reducing computational requirements.

In the same year, Wang et al. (2006) presented results from a study carried out to assess the effect of stent and balloon geometrical properties, such as strut width and balloon length, on the transient behaviour of two study-specific stents during free expansion. The balloon was modelled as an idealised cylinder and the expansion of the stents was achieved through the application of a pressure load on their inner surface. It was observed that varying the proximal and distal strut width and the balloon length had a significant effect on the degree of dog-boning exhibited by each stent during free expansion. It was stated by the authors that a zero-shortening stent could conceivably be designed through the control of these parameters and through the adjustment of the position of the links in the stent geometry. To validate the results of the numerical analysis, the transient behaviour of the modelled stents was compared to that of several real stents expanded through balloon dilation. Although the real stents were longer than the modelled stents (17 mm vs. 10 mm), similar expansion profiles were observed between a number of the modelled stents and their experimental counterparts.

De Beule et al. (2008) presented results from a study carried out to compare the transient behaviour of a Bx-Velocity stent during free expansion achieved through three different loading scenarios. In the first simulation, the expansion of the stent was achieved through the application of a pressure load directly on the inner surface of the stent. In the second simulation, expansion of the stent was achieved through the application of a displacement-driven loading condition on the inner surface of an idealised cylindrical balloon. In the final simulation, the expansion of the stent was modelled through the application of a pressure load on the inner surface of a sophisticated model of a tri-folded catheter balloon. It was observed that the transient behaviour of the stent was highly dependent on the loading scenario employed to simulate its expansion (Figure 4). Ignoring the presence of a balloon in the expansion of the

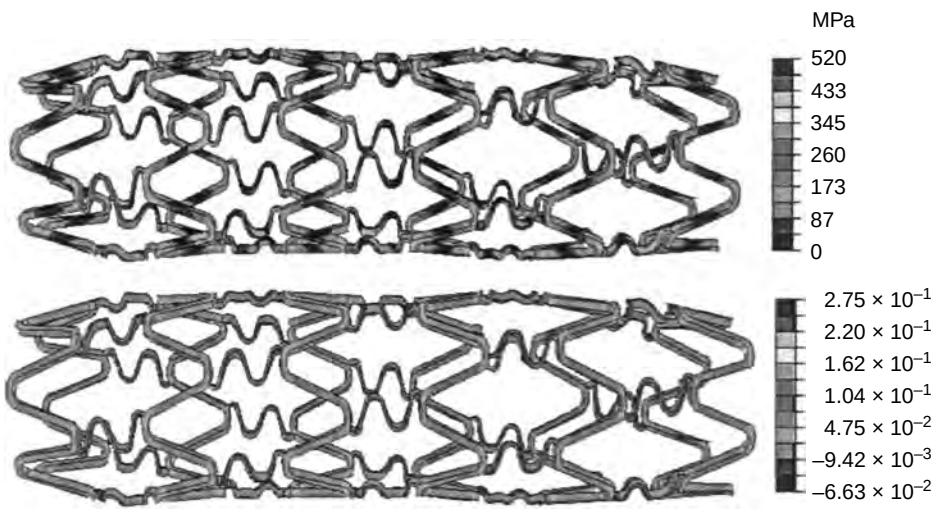

Figure 3. Von Mises stresses at an inflating pressure of 0.5 MPa (top) and equivalent plastic deformation after the load removal (bottom; Migliavacca et al. 2005).

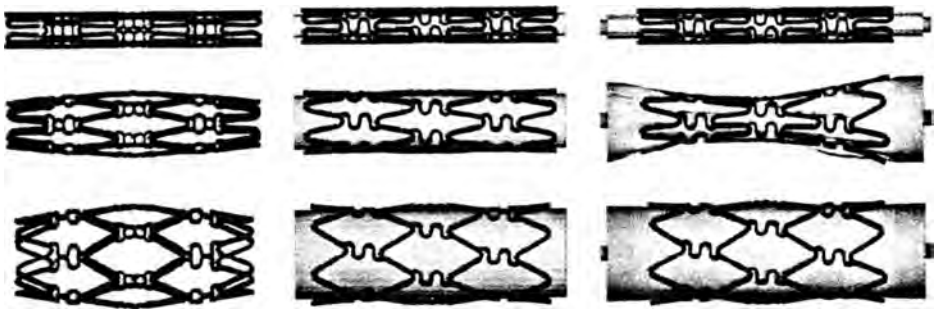

Figure 4. Stent deployment patterns resulting from the application of a pressure load on the stent inner surface (left), a displacement-driven loading condition on an idealised cylindrical balloon (middle) and a pressure load on the inner surface of a tri-folded balloon (right), prior to (top), during (centre) and after (bottom) free expansion (De Beule et al. 2008).

stent leads to an unrealistic expansion profile characterised by larger radial displacements in the central section of the stent compared with its extremities. In the second loading scenario, the profile of the stent was characterised by the displacement-driven expansion of an idealised cylindrical balloon and, as such, no bulging or dog-boning effects were observed. Only the simulation which incorporated the actual folded shape of the balloon was capable of capturing the dog-boning of the stent during its free expansion. The results of the simulations were validated against the manufacturers' data and it was noted that accounting for the presence of the folded balloon ensured an extremely close agreement between the predicted and the manufacturers' pressure–diameter measurements.

Lim et al. (2008) presented results from a study of the deployment characteristics of several stents during free expansion. The aim of the study was to identify potential stent design parameters capable of reducing the possibility of ISR driven by foreshortening and dog-boning. Three-dimensional numerical models of seven commercially available stents and a tri-folded catheter balloon were generated and considered in the study. Interestingly, the catheter balloon was discretised using a number of shell and fluid elements and the expansion of each stent was then achieved through a volume control process. Validation of this approach was performed by comparing predicted pressure–diameter relationships to experimental data reported in the literature (Dumoulin and Cochelin 2000; Migliavacca et al. 2005; Wang et al. 2006). Similar expansion profiles were observed for each stent, and predicted rates of foreshortening and dog-boning were measured. The authors noted that rates of foreshortening and dog-boning were generally higher among stents comprising closed unit cells connected by straight-line link elements as opposed to open unit cells connected by bend-shaped link structures.

3.2 *FE analysis of stent deployment within a vessel*

To date, several studies have been carried out to investigate how geometrical properties, material properties and deployment methods affect the expansion characteristics and biomechanical impact of stents when deployed within both normal and occluded coronary arteries (Auricchio et al. 2001; Berry et al. 2002; Prendergast et al. 2003; Chua et al. 2004b; Migliavacca et al. 2004; Holzapfel, Stadler, Gasser 2005; Lally et al. 2005; Liang et al. 2005; Walke et al. 2005; Ballyk 2006; Bedoya et al. 2006; Marrey et al. 2006; Kiousis et al. 2007; Takashima et al. 2007; Timmins et al. 2007; Wu et al. 2007b, 2007c; Gervaso et al. 2008; Gijsen et al. 2008; Capelli et al. 2009; Early et al. 2009; Pericevic et al. 2009). A number of studies that represent significant contributions to research in this field are discussed and summarised in this section (Table 2).

Auricchio et al. (2001) presented results from a study carried out to investigate the deployment characteristics of a Palmaz–Schatz stent when expanded within an idealised stenotic artery. The stenotic artery was modelled as a cylindrical vessel with a parabola-shaped plaque. Both the artery and the plaque were simplified as isotropic, homogeneous, incompressible materials and their material behaviour was defined using hyperelastic constitutive material models based on data reported in the literature (Hayashi and Imai 1997). The expansion of the stent was achieved through the application of a pressure load on its inner surface and a number of stent deployment characteristics such as elastic recoil, foreshortening and metal-to-artery-ratio surface ratio were calculated. This study represents one of the first attempts to utilise the FE method to analyse the expansion of a stent within a stenotic artery.

Chua et al. (2004b) presented results from a study carried out to evaluate the deployment characteristics of a Palmaz–Schatz stent when expanded within an idealised stenotic artery and to assess the degree of stent-induced arterial stresses incurred in the vessel. The stenotic artery was modelled as a cylindrical vessel with a parabola-shaped plaque. Both the artery and the plaque were simplified as homogenous, isotropic and incompressible materials and their behaviour was defined using linear elastic material models based on data reported in the literature (Veress et al. 2000). The expansion of the stent was achieved through the

Table 2. Finite element studies of stent deployment within a vessel.

Years	Authors	Study title	Modelling parameters	Study aims and conclusions
2001	Auricchio et al. (2001)	FE analysis of a stenotic revascularisation through a stent insertion	*Stent model*: Palmaz–Schatz stent *Stent material model*: elastic–plastic model based on properties of 316L stainless steel *Artery model*: cylindrical artery with ideal plaque *Artery material model*: hyperelastic models based on data reported in the literature (Hayashi and Imai 1997) *Solver type*: implicit (ABAQUS©/Standard)	*Aim*: to investigate the deployment characteristics of a Palmaz–Schatz stent when expanded within an idealised stenotic artery *Conclusions*: numerical results were validated against experimental data in the literature proving that the deployment of a stent within a vessel may be accurately simulated using the FE method
2004	Chua et al. (2004b)	FE simulation of slotted tube (stent) with the presence of plaque and artery by balloon expansion	*Stent model*: Palmaz–Schatz stent *Stent material model*: elastic–plastic model based on properties of 304 stainless steel *Balloon model*: cylindrical balloon *Balloon material model*: hyperelastic model based on properties of polyurethane rubber *Artery model*: cylindrical artery with ideal plaque *Artery material model*: linear elastic models based on data reported in the literature (Veress et al. 2000) *Solver type*: explicit (ANSYS©/LS-DYNA)	*Aim*: to evaluate the deployment characteristics of a Palmaz–Schatz stent when expanded within an idealised stenotic artery and to assess the degree of stent-induced arterial stresses incurred in the vessel *Conclusions*: maximum predicted stresses were concentrated in regions which coincide with locations at which plaque rupture is most predominantly reported
2005	Lally et al. (2005)	Cardiovascular stent design and vessel stresses: a FE analysis	*Stent model*: NIR and S7 stents *Stent material model*: linear elastic model based on properties of 316L stainless steel *Artery model*: cylindrical artery with ideal plaque *Artery material model*: hyperelastic models based on data reported in the literature (Loree et al. 1994; Prendergast et al. 2003) *Solver type*: implicit (MSC Marc©)	*Aim*: to investigate the effect of two different stent designs on the degree of stent-induced arterial stresses in an idealised stenotic artery *Conclusions*: a correlation was observed between the predicted volume of the arterial vessel subject to high levels of stent-induced stresses and the reported ISR rates for both stents
2005	Liang et al. (2005)	FE analysis of the implantation of a balloon-expandable stent in a stenosed artery	*Stent model*: study-specific stent design *Stent material model*: elastic–plastic model based on properties of 316L stainless steel *Balloon model*: cylindrical balloon *Balloon material model*: hyperelastic model based on experimental data *Artery model*: cylindrical artery and plaque *Artery material model*: hyperelastic and visco-plastic material models *Solver type*: implicit (ANSYS©)	*Aim*: to evaluate the deployment characteristics of a study-specific stent when expanded within an idealised stenotic artery and to assess the degree of stent-induced arterial stresses incurred in the vessel *Conclusions*: stent deployment induced high stress concentrations on sections of the artery that coincide with common sites at which ISR tends to be prevalent

Table 2 – *continued*

Years	Authors	Study title	Modelling parameters	Study aims and conclusions
2005	Holzapfel, Stadler, Gasser (2005)	Changes in the mechanical environment of stenotic arteries during the interaction with stents	*Stent model*: Multi-Link, Niroyal Elite and InFlow Gold stents *Stent material model*: elastic–plastic model based on properties of 316L stainless steel *Artery model*: patient-specific artery with stenosis *Artery material model*: hyperelastic models based on data reported in the literature (Holzapfel et al. 2000, 2002, 2004) *Solver type*: implicit (not disclosed)	*Aim*: to investigate the effect of various geometrical parameters on the biomechanical impact of three different stents when expanded within a realistic, patient-specific model of a stenotic artery *Conclusions*: it is possible to assess the deployment of a stent within a realistic, patient-specific artery using magnetic resonance imaging and a number of constitutive material models
2006	Bedoya et al. (2006)	Effects of stent design parameters on normal artery wall mechanics	*Stent model*: study-specific stent design *Stent material model*: elastic–plastic model based on properties of 316L stainless steel *Artery model*: cylindrical artery *Artery material model*: hyperelastic model based on experimental data *Solver type*: implicit (MSC Marc©)	*Aim*: to evaluate the effect of geometrical properties on the deployment characteristics of a study-specific stent when expanded within an idealised normal *Conclusions*: large stent strut-spacing, radius of strut curvature and axial ring amplitude are associated with lower levels of stent-induced arterial stress
2007	Wu et al. (2007c)	Stent expansion in a curved vessel and their interactions: an FE analysis	*Stent model*: study-specific stent design *Stent material model*: elastic–plastic model based on properties of 316L stainless steel *Artery model*: straight and curved idealised cylindrical arteries *Artery material model*: hyperelastic models based on data reported in the literature (Lee 2000) *Solver type*: implicit (ANSYS©)	*Aim*: to evaluate the biomechanical impact of a study-specific stent when deployed within both straight and curved idealised stenotic arteries *Conclusions*: the deployment of the study-specific stent within the curved stenotic artery straightened the vessel inducing high stresses in the plaque and in the arterial wall
2008	Gervaso et al. (2008)	On the effects of different strategies in modelling balloon-expandable stenting by means of FE method	*Stent model*: Bx-Velocity stent *Stent material model*: elastic–plastic model based on properties of 316L stainless steel *Balloon model*: tapered balloon *Balloon material model*: linear elastic model based on manufacturer's data *Artery material model*: hyperelastic material models based on data reported in the literature (Holzapfel, Sommer, Gasser, Regitnig 2005) *Artery model*: tri-layer cylindrical artery *Solver type*: explicit (ABAQUS©/Explicit)	*Aim*: to compare and contrast the degree of arterial stress induced in an idealised normal artery following the deployment of a Bx-Velocity stent simulated by three different loading scenarios *Conclusion*: predicted distributions of stent-induced arterial stresses are highly dependent on the loading scenario employed to simulate the expansion of the stent

Table 2 – *continued*

Years	Authors	Study title	Modelling parameters	Study aims and conclusions
2008	Gijsen et al. (2008)	Simulation of stent deployment in a realistic human coronary artery	*Stent model*: Bx-Velocity stent *Stent material model*: elastic–plastic model based on properties of 316L stainless steel *Artery model*: patient-specific artery with stenosis *Artery material model*: hyperelastic material models based on experimental data *Solver type*: implicit (ABAQUS©/Standard)	*Aim*: to investigate the effect of stent deployment on stresses and strains in both a stent and the vessel wall of a realistic, patient-specific model of a stenotic artery *Conclusions*: Predicted arterial stresses were concentrated behind stent struts and where the thickness of the arterial wall was a minimum. Peak stresses were coincident with locations where increased neointimal hyperplasia is generally observed. Stress levels and distribution were similar for increased strut thickness but required increased inflation pressure
2009	Capelli et al. (2009)	Assessment of tissue prolapse after balloon-expandable stenting: influence of stent cell geometry	*Stent model*: Bx-Velocity, Carbostent, JoStent and Multi-Link stents *Stent material model*: elastic–plastic model based on properties of 316L stainless steel *Balloon model*: tapered balloon *Balloon material model*: linear elastic model based on manufacturer's data *Artery model*: tri-layer cylindrical artery *Artery material model*: hyperelastic material models based on data reported in the literature (Holzapfel, Sommer, Gasser, Regitnig 2005) *Solver type*: explicit (ABAQUS©/Explicit)	*Aim*: to assess the influence of stent cell geometry on the degree of arterial tissue prolapse observed during stent deployment within an idealised normal artery *Conclusions*: the highest measure of tissue prolapse among the five stents considered was observed in the Carbostent model which coincidentally had the highest printed area (the greatest inscribable convex quadrilateral in the expanded stent cell)
2009	Pericevic et al. (2009)	The influence of plaque composition on underlying arterial wall stress during stent expansion: the case for plaque-specific stents	*Stent model*: Driver stent *Stent material model*: elastic–plastic model based on properties of MP35N cobalt alloy *Artery model*: cylindrical artery and plaque *Artery material model*: hyperelastic models based on data reported in the literature (Loree et al. 1994; Lally et al. 2004) *Solver type*: explicit (ANSYS©/LS-DYNA)	*Aim*: to evaluate the influence of plaque composition on the degree of underlying arterial stresses induced following deployment of a Driver stent within an idealised stenotic artery *Conclusions*: the material properties of a plaque have a significant influence on the underlying arterial stresses induced during stent deployment with stiffer plaques playing a protective role during stent deployment

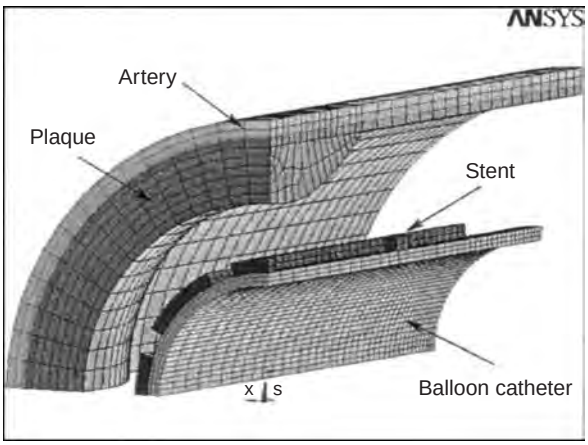

Figure 5. Numerical model of the balloon-stent-plaque-artery assembly (Chua et al. 2004b).

application of a pressure load on the inner surface of an idealised cylindrical balloon (Figure 5). It was observed by the authors that the regions which were subject to the highest stresses in the stenotic artery coincided with locations at which most plaque ruptures have been reported. Deployment characteristics of the stent were also reported and it was observed that the maximum diameter achieved when the stent was expanded within the stenotic artery was significantly less than the maximum diameter achieved by the stent during free expansion. Although the behaviour of the stenotic artery was idealised using linear elastic material models, the results obtained demonstrate the possible regions of high stresses that may be induced during stent deployment within a stenotic artery.

Lally et al. (2005) presented results from a study carried out to investigate the effect of two different stent designs on the degree of stent-induced arterial stresses in an idealised stenotic artery. The stents considered were based on the expanded configuration of the S7 (Medtronic AVE, Minneapolis, MN, USA) and NIR stents. Again, the stenotic artery was modelled as a cylindrical vessel with a parabola-shaped plaque. Both the artery and the plaque were simplified as homogenous, isotropic and incompressible materials and their behaviour was defined using hyperelastic constitutive material models based on data reported in the literature (Loree et al. 1994; Prendergast et al. 2003). To simulate the expansion of the stent within the stenotic artery, a two-step procedure was employed. First, the stent elements were deactivated and the vessel was expanded to a diameter greater than that of the stent through the application of a sufficient pressure load on its inner surface. In the second step, the stent elements were reactivated and the pressure load on the inner surface of the vessel was gradually reduced to a value corresponding with mean blood pressure. It was observed that the NIR stent subjected significantly larger volumes (21 vs. 4%) of the vessel to high tensile stresses (>4 MPa). A correlation was observed between the volume of the arterial vessel subject to high levels of stent-induced stresses and the reported ISR rates for the both stents. The results of this study again highlight the potential of the FE method in the design and optimisation of coronary stents.

Liang et al. (2005) presented results from a study carried out to evaluate the deployment characteristics of a study-specific stent when expanded within an idealised stenotic artery and to assess the degree of stent-induced arterial stresses incurred in the vessel. The stenotic artery was modelled as a cylindrical vessel with a cylinder-shaped plaque. Both the artery and the plaque were simplified as homogenous, isotropic and incompressible materials and their behaviour was defined using hyper-elastic constitutive material models. The constitutive model for the arterial tissue was derived from experimental testing of human arterial tissue, while a novel visco-plastic material model was established for the plaque to simulate both the elastic deformation of the plaque itself and the non-elastic deformation of the interlining between the plaque and the artery. The authors state that this is clearly a limiting assumption due to the lack of experimental data. The expansion of the stent within the vessel was achieved through the application of a pressure load on the inner surface of an idealised cylindrical balloon. The distribution of stress within both the stent and the vessel and the rate of elastic recoil of the stent when expanded with and without the presence of the vessel were reported. It was observed that, as the length of the stent was greater than that of the plaque, its extremities tilted during its deployment. This resulted in high stress concentrations in the corresponding section of the arterial wall and it was noted by the authors that the areas in question coincide with common sites at which ISR tends to occur in clinical practice.

In the same year, Holzapfel, Stadler, Gasser (2005) presented results from a study carried out to investigate the effect of various geometrical parameters such as stent cell dimensions and strut thickness on the biomechanical impact of three different stents when expanded within a realistic, patient-specific model of a stenotic artery. Three stent designs were considered in the study and were based on the Multi-Link, NIR and InFlow Gold (Boston Scientific) stents. A realistic model of a stenotic artery was generated using magnetic resonance images of an actual iliac artery. The properties of several sections of the stenotic artery were defined using a number of hyperelastic constitutive material models based on experimental data reported in the literature (Holzapfel et al. 2000, 2002, 2004). The expansion of the stents within the vessel was achieved through the application of a pressure load on their inner surface. The results of this study were used to investigate the influence of mismatch, strut thickness and cell geometry on intimal pressure concentrations and the degree of stent-induced arterial stresses. Although the authors noted that the conclusions drawn in the study are

relevant only for the considered stenotic artery, this study highlights the potential of the FE method in simulating stent expansion within realistic, patient-specific stenotic vessels.

Bedoya et al. (2006) presented results from a study carried out to evaluate the effect of geometrical parameters such as axial strut spacing, ring amplitude and strut radius of curvature on the deployment characteristics of a study-specific stent when expanded within an idealised normal artery and to assess the degree of stent-induced arterial stresses incurred in the vessel. The artery was modelled as a homogenous, isotropic and incompressible cylindrical vessel and its behaviour was defined using a hyperelastic constitutive material model based on the results of pressure–diameter and force–elongation tests carried out on a porcine carotid artery. The expansion of the stent within the vessel was achieved using a similar strategy to that reported by Lally et al. (2005) and it was observed that the deployment characteristics and the degree of stent-induced arterial stresses were strongly affected by the geometrical features of the stent. It was noted that, of the stents considered, the one which incorporated the largest strut spacing, ring amplitude and radius of strut curvature was superior to the other stents in terms of reduced stent-induced arterial stresses. Timmins et al. (2007) extended the work of Bedoya et al. (2006) by developing a numerical subroutine to optimise the design of the stent based on its performance when deployed within a normal artery. Based on the numerical results, single parameter outputs derived from the predicted levels of stent-induced arterial stress, lumen gain and cyclic deflection were defined and utilised in an optimisation algorithm developed to automatically generate improved stent geometries. These studies further highlight the potential of the FE method in the optimisation of coronary stents design.

Wu et al. (2007c) presented results from a study carried out to evaluate the biomechanical impact of a study-specific stent when deployed within both straight and curved stenotic arteries. The straight vessel was modelled as an idealised cylinder with a parabola-shaped plaque, while the curved vessel was modelled in an identical fashion but defined with a curvature of $0.1\ \mathrm{mm}^{-1}$ in a toroidal coordinate system. Both the arterial tissue and the plaque were simplified as homogenous, isotropic and incompressible materials and their behaviour was defined using hyperelastic constitutive material models based on data reported in the literature (Lee 2000). To simulate the expansion of the stent in the curved vessel, contact was initially deactivated and a pressure load was applied to the inner surface of the vessel causing it to expand to a diameter greater than the expanded diameter of the stent. Next, all deactivated contact elements were reactivated and the expansion of the stent was achieved through the application of a displacement-driven boundary condition on a cylindrical analytical surface. Once the stent had been expanded, the pressure load on the vessel was gradually reduced to that of mean blood pressure. According to the authors, the stent completely failed to conform to the shape of the curved vessel, causing it to straighten inducing high levels of stress in the plaque at the point of inner curvature and in the arterial wall at its outer extremities. The maximum stress recorded in the curved vessel was three times that predicted in the straight vessel and it was concluded by the authors that the non-conformity of the stent was due to insufficient deformation of its link segments, especially at the extremities of the stent.

The following year, Gervaso et al. (2008) presented results from a study carried out to compare and contrast the degree of arterial stress induced in a normal artery following the deployment of a Bx-Velocity stent achieved through three different loading scenarios. The artery was modelled as an idealised cylinder and partitioned into three layers of equal thickness, representing the tunica intima, media and adventitia. These individual tissues were simplified as homogenous and incompressible materials and their behaviour was defined using hyperelastic constitutive material models based on data reported in the literature (Holzapfel, Sommer, Gasser, Regitnig 2005). In the first simulation, the expansion of the stent was achieved through the application of a pressure load directly on the inner surface of the stent. In the second simulation, expansion of the stent was achieved through the application of a displacement-driven loading condition on the inner surface of an idealised cylindrical balloon. In the final simulation, the expansion of the stent was modelled through the application of a pressure load on the inner surface of a deflated, tapered catheter balloon. It was observed that the predicted distribution of stent-induced arterial stress is highly dependent on the loading scenario employed to simulate the expansion of the stent. Simulation of the tapered balloon resulted in a more diffuse distribution of circumferential and radial stresses in the vessel wall, and based on this observation the authors concluded that realistic balloon modelling is essential for accurately predicting the degree of arterial injury caused during stent placement.

In same year, Gijsen et al. (2008) presented results from a study carried out to investigate the biomechanical impact of a Bx-Velocity stent when expanded within a realistic, patient-specific model of a stenotic artery. This realistic arterial model was generated based on biplane angiography and intravascular ultrasound measurements of an actual borderline stenotic right coronary artery. The artery was modelled as a homogenous, isotropic and incompressible material and its behaviour was defined using a hyperelastic constitutive material model. It was noted that the stress–strain relationship defined by this model was typical of that reported in the literature (Prendergast et al. 2003; Holzapfel, Sommer, Gasser, Regitnig 2005). The stent was appropriately positioned within the vessel and its expansion was achieved through the application of a pressure load on its inner surface. It was observed by Gijsen et al. that due to the

tapered nature of the vessel, larger dilation of the stent was achieved in the proximal section of the artery where the pre-expansion lumen diameter was highest. Predicted arterial stresses were concentrated in the region coincident to the stent struts and where the thickness of the vessel wall was a minimum. It was also noted that the predicted stresses coincided well with locations where increased neointimal hyperplasia is generally observed. The methodology developed in this study was proposed as a preclinical evaluation tool for the identification of optimal stent designs for the treatment of patients on a lesion-specific basis.

Capelli et al. (2009) presented results from a study carried out to assess the influence of stent cell geometry on the degree of arterial tissue prolapse observed during stent deployment within an idealised normal artery. Five different stents were considered and were based on the Palmaz–Schatz, Bx-Velocity, Multi-Link, Jostent Flex (JoMed, Helsingborg, Sweden) and Carbostent stents. Again, the artery was modelled as a cylinder and partitioned into three layers of equal thickness, representing the tunica intima, media and adventitia. The arterial tissues were simplified as homogenous and incompressible materials and their behaviour was defined using hyper-elastic constitutive material models based on data reported in the literature (Holzapfel, Sommer, Gasser, Regitnig 2005). The expansion of each stent was achieved through the application of a pressure load on the inner surface of a deflated, tapered catheter balloon. Once the stent had been deployed, the stresses induced in the arterial wall and the degree of tissue prolapsed within the stent cells were evaluated. Similar distributions of stent-induced arterial stresses were observed for each of the five stents and the highest measure of tissue prolapse, expressed in terms of radial recoil and printed area (the greatest inscribable convex quadrilateral in the expanded stent cell), was observed in the Carbostent model, which coincidentally had the highest printed area. The results of this study further underline the importance of stent geometrical properties in the optimisation of stent design.

Also Pericevic et al. (2009) presented results from a study carried out to evaluate the influence of plaque composition on the degree of underlying arterial stresses induced following the deployment of a Driver stent (Medtronic AVE) within an idealised stenotic artery. The stenotic artery was modelled as a cylindrical vessel with a parabola-shaped plaque. Both the artery and the plaque were simplified as homogenous and incompressible materials and their behaviour was defined using hyper-elastic constitutive material models. The constitutive model for the arterial tissue was based on data reported in the literature while separate constitutive models, also derived from data reported in the literature, were introduced for three different classifications of athero-sclerotic tissue (cellular, hypercellular and calcified; Loree et al. 1994; Lally et al. 2004). The expansion of the stent was achieved through the application of a pressure load ranging from 0 atm to either 9, 12 or 15 atm on its inner surface, and it was observed that the material properties of the plaque had a significant influence on the stresses induced in the underlying arterial tissue. Overall, the highest stresses were predicted in the vessel with the hypercellular plaque, while the stiffer calcified plaque appeared to play a protective role in the vessel, reducing the levels of stress observed within the underlying tissue

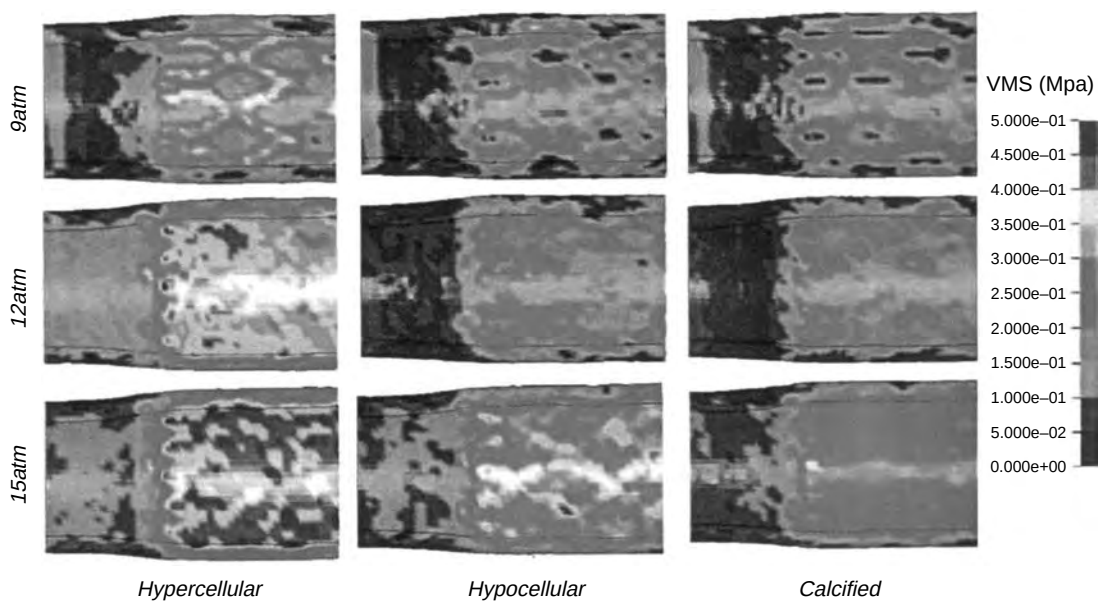

Figure 6. Von Mises stress distribution in a normal artery as a function of plaque classification following stent deployment at three different pressure loads (Pericevic et al. 2009).

(Figure 6). The results of this study suggest that higher pressures could be applied to calcified plaques during stent expansion with a lower risk of arterial injury.

4. Conclusion

Computational numerical methods such as the FE method have emerged as essential and widely adopted tools for the assessment and optimisation of biomedical devices such as coronary stents. To date, the FE method has been utilised in a large number of studies to investigate both the structural properties of stents and their biomechanical impact on the coronary artery during deployment. Over the past decade, rapidly increasing levels of computational power have led to considerable increases in the level of complexity and sophistication involved in these studies. Today, elaborate models of commercially available stents, tri-folded catheter balloons and stenotic arteries are the norm, while the idealised material models initially used to describe the behaviour of complicated biological tissues have been superseded by sophisticated hyperelastic constitutive material models. The development of this research over the last decade has been thoroughly reviewed in this paper by highlighting the contribution of a number of key studies in this field.

In the coming years, advances in the numerical analysis of coronary stents should allow for more work to be carried out with patient-derived arterial models. Although simplified approaches have contributed enormously to the current level of understanding of the structural properties of coronary stents, there is a need to investigate the performance of these devices within realistic models of stenosed arteries. To the best of the authors' knowledge, only the work of Holzapfel et al, Kiousus et al. and Gijsen et al. have utilised patient-derived arterial geometries in the structural analysis of stent deployment. These studies provide a deep insight into the response of an actual stenosed vessel under the supra-physiological loading conditions induced during stent placement. The use of patient-derived arterial models in conjunction with constitutive material models, capable of capturing the non-linear, anisotropic behaviour of diseased and non-diseased arterial tissue, has the potential to provide a scientific basis for the identification and optimisation of suitable stent geometries and materials in the treatment of CAD on a patient-specific basis.

Also, as DESs continue to succeed BMSs in the treatment of CAD, future advances in the numerical analysis of coronary stents will likely involve the coupling of the FE method with other numerical methods such as computational fluid dynamics and mass transport analysis. Through the coupling of these numerical methods, as displayed by the promising work of Zunino et al. (2009), comprehensive models for the evaluation of stent performance in terms of its deployment characteristics influence on local vessel haemodynamics and effective drug-release may be developed. Furthermore, as bioabsorbable coronary stents such as the BVS everolimus-eluting stent (Abbott Vascular, Santa Clara, CA, USA) continue to perform well in clinical evaluation (Serruys et al. 2009), sophisticated numerical models capable of predicting both device degradation and drug-release from the device, such as that proposed by Perale et al. (2009) will be required. It is possible that the development, adoption and coupling of each of these numerical methods may one day lead to their direct incorporation in clinical practice.

References

Auricchio F, Di Loreto M, Sacco E. 2001. Finite element analysis of a stenotic artery revascularisation through a stent insertion. Comput Methods Biomech Biomed Eng. 4: 249–263.

Ballyk P. 2006. Intramural stress increases exponentially with stent diameter: a stress threshold for neointimal hyperplasia. J Vasc Interv Radiol. 17:1139–1145.

Balossino R, Gervaso F, Migliavacca F, Dubini D. 2008. Effects of different stent designs on local hemodynamics in stented arteries. J Biomech. 41:1053–1061.

Bedoya J, Meyer C, Timmins L, Moreno M, Moore Jr. J. 2006. Effects of stent design parameters on normal artery wall mechanics. J Biomech Eng. 128:757–765.

Berry J, Manoach E, Mekkaoui C, Rolland P, Moore Jr. J, Rachev A. 2002. Hemodynamics and wall mechanics of a compliance matching stent: *in vitro* and *in vivo* analysis. J Vasc Interv Radiol. 13:97–105.

Brauer H, Stolpmann J, Hallmann H, Erbel R, Fischer A. 1999. Measurement and numerical simulation of the dilatation behaviour of coronary stents. Materwiss Werksttech. 40: 876–885.

Capelli C, Gervaso F, Petrini L, Dubini G, Migliavacca F. 2009. Assessment of tissue prolapse after balloon-expandable stenting: influence of stent cell geometry. Med Eng Phys. 31: 441–447.

Chua D, MacDonald B, Hashmi M. 2002. Finite-element simulation of stent expansion. J Mater Process Technol. 120:335–340.

Chua D, MacDonald B, Hashmi M. 2003. Finite element simulation of stent and balloon interaction. J Mater Process Technol. 143–144:591–597.

Chua D, MacDonald B, Hashmi M. 2004a. Effects of varying slotted tube (stent) geometry on its expansion behaviour using finite element method. J Mater Process Technol. 155–156:1764–1771.

Chua D, MacDonald B, Hashmi M. 2004b. Finite element simulation of slotted tube (stent) with the presence of plaque and artery by balloon expansion. J Mater Process Technol. 155–156:1772–1779.

Daemen J, Wenaweser P, Tsuchida K, Abrecht L, Vaina S, Morger C, Kukreja N, Jüni P, Sianos G, Hellige G, et al. 2007. Early and late coronary stent thrombosis of sirolimus-eluting and paclitaxel-eluting stents in routine clinical practice: data from a large two-institutional cohort study. Lancet. 369:667–678.

De Beule M, Mortier P, Belis J, Van Impe R, Verhegghe B, Verdonck P. 2007. Plasticity as a lifesaver in the design of cardiovascular stents. Key Eng Mater. 340–341:841–846.

De Beule M, Mortier P, Carlier S, Verhegghe B, Van Impe R, Verdonck P. 2008. Realistic finite element-based stent design: the impact of balloon folding. J Biomech. 41: 383–389.

De Beule M, Mortier P, Van Impe R, Verhegghe B, Segers P, Verdonck P. 2007. Plasticity in the mechanical behaviour of cardiovascular stents during stent preperation (crimping) and placement (expansion). Key Eng Mater. 340–341:847–852.

Donnelly E, Bruzzi M, Connelly T, McHugh P. 2007. Finite element comparison of performance related characteristics of balloon-expandable stents. Comput Methods Appl Mech Eng. 10:103–110.

Dumoulin C, Cochelin B. 2000. Mechanical behaviour modelling of balloon-expandable stents. J Biomech. 33:1461–1470.

Dyet J, Watts W, Ettles D, Nicholson A. 2000. Mechanical properties of metallic stents: how do these properties influence the choice of stent for specific lesions? CardioVasc Intervent Radiol. 23:47–54.

Early M, Lally C, Prendergast P, Kelly DJ. 2009. Stresses in peripheral arteries following stent placement: a finite element analysis. Comput Methods Biomech Biomed Eng. 12:25–33.

Etave F, Finet G, Boivin M, Boyer J, Rioufol G, Thollet G. 2001. Mechanical properties of coronary stents determined by using finite element analysis. J Biomech. 34:1065–1075.

Finn A, Joner M, Nakazawa G, Kolodgie F, Newell J, John M, Gold H, Virmani R. 2007. Pathological correlates of late drug-eluting stent thrombosis: strut coverage as a marker of endothelialization. Circulation. 115:2435–2441.

Fischman D, Leon M, Baim D, Schatz R, Savage M, Penn I, Detre K, Veltri L, Ricci D, Nobuyoshi M, et al. 1994. The Stent Restenosis Study Investigators. A randomized comparison of coronary-stent placement and balloon angioplasty in the treatment of coronary artery disease. N Engl J Med. 331:496–501.

Gervaso F, Capelli C, Petrini L, Lattanzio S, Di Virgilio L, Migliavacca F. 2008. On the effects of different strategies in modelling balloon-expandable stenting by means of finite element method. J Biomech. 41:1206–1212.

Gijsen F, Migliavacca F, Schievano S, Socci L, Petrini L, Thury A, Wentzel J, van der Steen A, Serruys P, Dubini G. 2008. Simulation of stent deployment in a realistic human coronary artery. BioMed Eng OnLine. 7:23.

Gu L, Santra S, Mericle R, Kumar A. 2005. Finite element analysis of covered microstents. J Biomech. 38:1221–1227.

Hall G, Kasper E. 2006. Comparison of element technologies for modeling stent expansion. J Biomech Eng. 128:751–756.

Hayashi K, Imai Y. 1997. Tensile property of atheromatous plaque and an analysis of stress in atherosclerotic wall. J Biomech. 30:573–579.

Holzapfel G, Schulze-Bauer C, Stadler M. 2000. Mechanics of angioplasty: wall, balloon and stent. In: Mechanics in biology. Vol AMD-Vol. 242/BED-Vol. 46. New York: The American Society of Mechanical Engineers.

Holzapfel G, Sommer G, Gasser C, Regitnig P. 2005. Determination of layer-specific mechanical properties of human coronary arteries with nonatherosclerotic intimal thickening and related constitutive modeling. Am J Physiol Heart Circ Physiol. 289:H2048–H2058.

Holzapfel G, Sommer G, Regitnig P. 2004. Anisotropic mechanical properties of tissue components in human atherosclerotic plaques. J Biomech Eng. 126:657–665.

Holzapfel G, Stadler M, Gasser T. 2005. Changes in the mechanical environment of stenotic arteries during interaction with stents: computational assessment of parametric stent designs. J Biomech Eng. 127:166–180.

Holzapfel G, Stadler M, Schulze-Bauer C. 2002. A layer-specific three-dimensional model for the simulation of balloon angioplasty using magnetic resonance imaging and mechanical testing. Ann Biomed Eng. 30:753–767.

Ju F, Xia Z, Sasaki K. 2008. On the finite element modelling of balloon-expandable stents. J Mech Behav Biomed Mater. 1: 86–95.

Kiousis D, Gasser T, Holzapfel G. 2007. A numerical model to study the interaction of vascular stents with human atherosclerotic lesions. Ann Biomed Eng. 35:1857–1869.

LaDisa J, Hettrick D, Olson L, Guler I, Gross E, Kress T, Kersten J, Warltier D, Pagel P. 2002. Stent implantation alters coronary artery hemodynamics and wall shear stress during maximal vasodilation. J Appl Physiol. 93:1939–1946.

LaDisa J, Olson L, Guler I, Hettrick D, Audi S, Kersten J, Warltier D, Pagel P. 2004. Stent design properties and deployment ratio influence indexes of wall shear stress: a three-dimensional computational fluid dynamics investigation within a normal artery. J Appl Physiol. 97:424–430.

LaDisa J, Olson L, Molthen R, Hettrick D, Pratt P, Hardel M, Kersten J, Warltier D, Pagel P. 2005. Alterations in wall shear stress predict sites of neointimal hyperplasia after stent implantation in rabbit iliac arteries. Am J Physiol Heart Circ Physiol. 288:H2465–H2475.

Lally C, Reid A, Prendergast P. 2004. Elastic behavior of porcine coronary artery tissue under uniaxial and equibiaxial tension. Ann Biomed Eng. 32:1355–1364.

Lally C, Dolan F, Prendergast P. 2005. Cardiovascular stent design and vessel stresses: a finite element analysis. J Biomech. 38:1574–1581.

Lee R. 2000. Atherosclerotic lesion mechanics versus biology. Z Kardiol. 89:S080–S084.

Li N, Zhang H, Ouyang H. 2009. Shape optimization of coronary artery stent based on a parametric model. Finite Elem Anal Des. 45:468–475.

Liang D, Yang D, Qi M, Wang W. 2005. Finite element analysis of the implantation of a balloon-expandable stent in a stenosed artery. Int J Cardiol. 104:314–318.

Lim D, Cho S-K, Park W-P, Kristensson A, Ko J-Y, Al-Hassani S, Kim H-S. 2008. Suggestion of potential stent design parameters to reduce restenosis risk driven by foreshortening or dogboning due to non-uniform balloon-stent expansion. Ann Biomed Eng. 36:1118–1129.

Lloyd-Jones D, Adams R, Carnethon M, De Simone G, Ferguson T, Flegal K, Ford E, Furie K, Go A, Greenlund K, et al. 2009. Heart disease and stroke statistics – 2009 update: a report from the American Heart Association Statistics Committee and Stroke Statistics Subcommittee. Circulation. 119:480–486.

Loree HM, Grodzinsky AJ, Park SY, Gibson LJ, Lee RT. 1994. Static circumferential tangential modulus of human atherosclerotic tissue. J Biomech. 27:195–204.

Mac Donald BJ. 2007. Practical stress analysis with finite elements. Glasnevin Publishing: Dublin.

Marrey R, Burgermeister R, Grishaber R, Ritchie R. 2006. Fatigue and life prediction for cobalt-chromium stents: a fracture mechanics analysis. Biomaterials. 27:1988–2000.

McGarry J, O'Donnell B, McHugh P, McGarry J. 2004. Analysis of the mechanical performance of a cardiovascular stent design based on micromechanical modelling. Comput Mater Sci. 31:421–438.

Migliavacca F, Petrini L, Colombo M, Auricchio F, Pietrabissa R. 2002. Mechanical behavior of coronary stents investigated through the finite element method. J Biomech. 35:803–811.

Migliavacca F, Petrini L, Massarotti P, Schievano S, Auricchio F, Dubini G. 2004. Stainless and shape memory alloy coronary stents: a computational study on the interaction with the vascular wall. Biomech Model Mechanobiol. 2:205–217.

Migliavacca F, Petrini L, Montanari V, Quagliana I, Auricchio F, Dubini G. 2005. A predictive study of the mechanical behaviour of coronary stents by computer modelling. Med Eng Phys. 27:13–18.

Morice M-C, Serruys P, Sousa J, Fajadet J, Ban Hayashi E, Perin M, Colombo A, Schuler G, Barragan P, Guagliumi G, et al. 2002. The RAVEL Study Group. A randomized comparison of a sirolimus-eluting stent with a standard stent for coronary revascularization. N Engl J Med. 346: 1773–1780.

Mortier P, De Beule M, Carlier S, Van Impe R, Verhegghe B, Verdonck P. 2008. Numerical study of the uniformity of balloon-expandable stent deployment. J Biomech Eng. 130: 021018.

Moses J, Leon M, Popma J, Fitzgerald P, Holmes D, O'Shaughnessy C, Caputo R, Kereiakes D, Williams D, Teirstein P, et al. 2003. The SIRIUS Investigators. Sirolimus-eluting stents versus standard stents in patients with stenosis in a native coronary artery. N Engl J Med. 349:1315–1323.

Ong A, van Domburg R, Aoki J, Sonnenschein K, Lemos P, Serruys P. 2006. Sirolimus-eluting stents remain superior to bare-metal stents at two years: medium-term results from the Rapamycin-Eluting Stent Evaluated at Rotterdam Cardiology Hospital (RESEARCH) registry. J Am Coll Cardiol. 47:1356–1360.

Perale G, Arosio P, Moscatelli D, Barri V, Müller M, Maccagnan S, Masi M. 2009. A new model of resorbable device degradation and drug release: transient 1-dimension diffusional model. J Control Release. 136:196–205.

Pericevic I, Lally C, Toner D, Kelly D. 2009. The influence of plaque composition on underlying arterial wall stress during stent expansion: the case for lesion-specific stents. Med Eng Phys. 31:428–433.

Petrini L, Migliavacca F, Auricchio F, Dubini G. 2004. Numerical investigation of the intravascular coronary stent flexibility. J Biomech. 37:495–501.

Pontrelli G, de Monte F. 2007. Modelling of mass convection-diffusion in stent-based drug-delivery. Paper presented at: XXV Congresso Nazionale UIT sulla Trasmssione del Calore; 18–20 May, 2007; Trieste.

Prendergast P, Lally C, Daly S, Reid A, Lee T, Quinn D, Dolan F. 2003. Analysis of prolapse in cardiovascular stents: a constitutive equation for vascular tissue and finite-element modelling. J Biomech Eng. 125:692–699.

Savage P, O'Donnell B, McHugh P, Murphy B, Quinn D. 2004. Coronary stent strut size dependent stress–strain response investigated using micromechanical finite element models. Ann Biomed Eng. 32:202–211.

Serruys P, Ormiston J, Onuma Y, Regar E, Gonzalo N, Garcia-Garcia H, Nieman K, Bruining N, Dorange C, Miquel-Hébert K, et al. 2009. A bioabsorbable everolimus-eluting coronary stent system (ABSORB): 2-year outcomes and results from multiple imaging methods. The Lancet. 373:897–910.

Stolpmann J, Brauer H, Stracke H, Erbel R, Fischer A. 2003. Practicability and limitations of finite element simulation of the dilation behaviour of coronary stents. Materwiss Werksttech. 34:736–745.

Stone GW, Ellis S, Cox D, Hermiller J, O'Shaughnessy C, Mann J, Turco M, Caputo R, Bergin P, Greenberg J, et al. 2004. The TAXUS-IV Investigators. A polymer-based, paclitaxel-eluting stent in patients with coronary artery disease. N Engl J Med. 350:221–231.

Takashima K, Kitou T, Mori K, Ikeuchi K. 2007. Simulation and experimental observation of contact conditions between stents and artery models. Med Eng Phys. 29:326–335.

Tan L, Webb D, Kormi K, Al-Hassani S. 2001. A method for investigating the mechanical properties of intracoronary stents using finite element numerical simulation. Int J Cardiol. 78:51–67.

Timmins L, Moreno M, Meyer C, Criscione J, Rachev A, Moore J. 2007. Stented artery biomechanics and device design optimization. Med Biol Eng Comput. 45:505–513.

Veress A, Vince D, Anderson PM. 2000. Vascular mechanics of the coronary artery. ASAJO. 89:II/92–II/100.

Vivek R, Stanley G. 2003. Coronary restenosis: a review of mechanisms and management. Am J Med. 115:547–553.

Walke W, Paszenda Z, Filipiak J. 2005. Experimental and numerical biomechanical analysis of vascular stent. J Mater Process Technol. 164–165:1263–1268.

Wang W-Q, Liang D-K, Yang D-Z, Qi M. 2006. Analysis of the transient expansion behavior and design optimization of coronary stents by finite element method. J Biomech. 39: 21–32.

Whitcher FD. 1997. Simulation of *in vivo* loading conditions of nitinol vascular stent structures. Comput Struct. 64: 1005–1011.

Wu W, Yang D, Qi M, Wang W. 2007a. An FEA method to study flexibility of expanded coronary stents. J Mater Process Technol. 184:447–450.

Wu W, Qi M, Liu X-P, Yang D-Z, Wang W-Q. 2007b. Delivery and release of nitinol stent in carotid artery and their interactions: a finite element analysis. J Biomech. 40: 3034–3040.

Wu W, Wang W-Q, Yang D-Z, Qi M. 2007c. Stent expansion in curved vessel and their interactions: a finite element analysis. J Biomech. 40:2580–2585.

Xia Z, Ju F, Sasaki K. 2007. A general finite element analysis method for balloon expandable stents based on repeated unit cell (RUC) model. Finite Elem Anal Des. 43:649–658.

Zunino P, D'Angelo C, Petrini L, Vergara C, Capelli C, Migliavacca F. 2009. Numerical simulation of drug eluting coronary stents: mechanics, fluid dynamics and drug release. Comput Methods Appl Mech Eng. 198:3633–3644.